arXiv:1408.3442v1 [cond-mat.mes-hall] 14 Aug 2014

Coulomb Interaction Effects on the Terahertz Photon-Assisted Tunneling through a InAs Quantum Dot

R.-Y. Yuan,[1] G.-B. Zhu,[2] X. Zhao,[3] Y. Guo,[4,5] H. Yan,[6] Q. Sun,[1,*] and A.-C. Ji[1,†]

[1]*Center for Theoretical Physics, Department of Physics, Capital Normal University, Beijing 100048, China*
[2]*Department of Physics, Heze University, Heze, Shandong 274015, China*
[3]*Department of Physics, Capital Normal University, Beijing 100048, China*
[4]*Department of Physics and State Key Laboratory of Low-Dimensional Quantum Physics, Tsinghua University, Beijing 100084, China*
[5]*Collaborative Innovation of Quantum Matter, Beijing, China*
[6]*Laboratory of Thin Film Materials, Beijing University of Technology, Beijing 100022, China*

(Dated: August 18, 2014)

Recently, the terahertz (THz) photon-assisted tunneling (PAT) through a two-level InAs quantum dot (QD) has been successfully realized in experiment [Phys. Rev. Lett. **109**, 077401 (2012)]. The Coulomb interaction in this device is comparable with the energy difference between the two energy levels. We theoretically explore the effects of Coulomb interaction on the PAT processes and show that the main peaks of the experiment can be well derived by our model analysis. Furthermore, we find additional peaks, which were not addressed in the InAs QD experiment and may be further identified in experiments. In particular, we show that, to observe the interesting photon-induced excited state resonance in InAs QD, the Coulomb interaction should be larger than THz photon frequency.

PACS numbers: 78.67.Hc, 07.57.Kp, 73.40.Gk

I. INTRODUCTION

In various nano-structures, such as a single electron transistor[1–3], applying a time varying oscillating potential to the Coulomb island can induce an inelastic tunneling event known as photon-assisted tunneling (PAT). PAT has been intensively studied, because it can be exploited to build a highly sensitive detector[4] or a solid-state quantum bit[5–8]. So far, these studies were mainly performed in the GHz range, namely microwave-field (MWF)[9–15]. On the other hand, the terahertz (THz) region, which is of fundamental industrial importance, has attracted broad scientific interest in the past decade[16,17]. However, the THz devices, especially in the region of 1-10 THz, have not been fully developed, giving rise to the so-called "THz gap".

Recently, experiments have been performed to implement a THz detector via the THz photon-assisted tunneling through a carbon nanotube[18,19] or self-assembled InAs quantum dot (QD)[20,21], where it was shown that both the charging and orbital quantization energies are typically 10-40 meV, which correspond to the THz region (2.5-10 THz). In the early works by the group of Ishibashi[18,19], the authors found that the carbon nanotubes QD can lead to new side peaks that appear only under the THz irradiations. Very recently, the THz PAT in a single self-assembled two-level InAs QD with s and p orbitals, has also been investigated by Shibata *et al.*[22]. They showed that, in addition to the PAT processes of s level and the Coulomb blockade oscillation of p level, an interesting photon-induced excited state resonance (PIER) of p level can be observed, when THz photon frequency is larger than the energy difference.

The irradiation induced PAT side peaks and the PIER in the presence of Coulomb blockade were first investigated in the MWF devices. Note that in a two-level MWF QD, the Coulomb interaction is much larger than the energy difference and regarded as infinite, all the Coulomb interaction related resonances are ignored[2]. Whereas in a InAs QD, because the energy difference lies in the THz region, the intra-dot Coulomb interaction becomes comparable with the energy difference. In this case, both the PAT and Coulomb blockade effects are involved together, and the finite Coulomb interaction may present new features on the resonant tunnelings beyond the MWF QD.

In this paper, we theoretically explore the Coulomb interaction effects on the PAT processes in InAs QD, see Fig. 1 for the schematic diagram. We demonstrate that, the presented peaks of our model analysis ε_s, $\varepsilon_p + U$, $\varepsilon_s \pm \omega$, ε_p agree well with E_0, E_1, $E_0 \pm hf_{\rm THz}$, and the PIER of p level in the experiment[22]. On the other hand, we find the side peak $\varepsilon_p - \omega$ induced by the THz irradiation in our model analysis. This peak can be identified in the original experimental data, but was not addressed in the reference[22]. In addition, beyond the Coulomb blockade oscillation peak $\varepsilon_p + U$, we also find there exists the $\varepsilon_s + U$ peak. This peak seems not readily discriminated from E_1 ($E_1 \equiv \varepsilon_p + U$) peak in the experiment. One may expect to identify both the peaks $\varepsilon_{s,p} + U$, which were not observed in the MWF QD due to infinite Coulomb interaction, by increasing the separation between the energies ε_s and ε_p in future experiment. In particular, we show that, to observe the interesting photon-induced excited state resonance of p level, the Coulomb interaction should be larger than THz photon frequency. These fea-

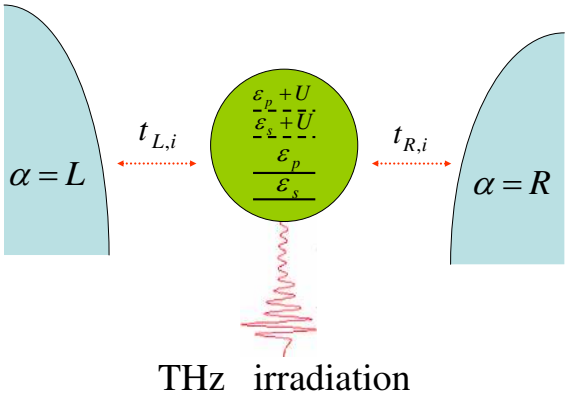

FIG. 1: (color online) Schematic diagram for the system of a two-level QD under the THz irradiation with frequency ω. Two reservoirs of 2DEG are connected with the center region, where $\varepsilon_{i=s,p}$ denotes the s and p energy levels in InAs QD. $t_{\alpha,i}$ describe the hopping matrix elements between leads and the two energy levels in the center region. U is the intra-dot Coulomb interaction and $\varepsilon_i + U$ are the Coulomb interaction related energy levels.

tures may be beneficial for future THz devices, such as an ultra-sensitive THz detector, which may also open new possibilities of controlling carrier dynamics in quantum nanostructures by THz radiation.

The organization of this paper is as follows: In Sec. II, we first present the tunneling model of the two-level InAs QD under THz irradiation. Then, we derive the formulation of average currents in Sec. III. In Sec. IV, we analyze the InAs QD experiment and explore the Coulomb interaction effects on the resonance tunnelings. Sec. V is the conclusion.

II. MODEL OF THE THZ PATS THROUGH A TWO-LEVEL QD

We consider a system of a two-level tunneling QD under the THz irradiation as depicted in Fig. 1, where $\varepsilon_{i=s,p}$ denotes the s and p energy levels in InAs QD. The dot is connected to two electronic reservoirs with chemical potentials μ_α, $\alpha = L, R$ and $\mu_L - \mu_R = eV$. Then, the Hamiltonian of the system can be described by

$$H(t) = H_{\rm lead} + H_{\rm d}(t) + H_{\rm t}, \tag{1}$$

where the first term $H_{\rm lead} = \sum_\alpha \varepsilon_{\alpha,k} c^\dagger_{\alpha,k} c_{\alpha,k}$ describes the left and right leads respectively. $\varepsilon_{\alpha,k}$ is the single-electron energy, and $c^\dagger_{\alpha,k}$ ($c_{\alpha,k}$) is the creation (annihilation) operator of the electrons in leads. The second term denotes the Hamiltonian of the central InAs QD, where we have taken into account the THz irradiation and intra-dot Coulomb interaction, which is given by

$$H_{\rm d}(t) = \sum_{i=s,p} \varepsilon_{d,i}(t) d^\dagger_i d_i + \frac{U}{2} n_i n_{\bar{i}}, \tag{2}$$

with $\varepsilon_{d,i}(t) = \varepsilon_i + W_d(t)$ denoting the time-dependent energy levels of the QD under the THz fields. Here, we have implemented the adiabatic approximation by introducing the THz irradiation as an oscillating potential with $W_d(t) = W_d \cos\omega t$[23,24], which causes a rigid shift of ε_i. $d^\dagger_i$ (d_i) is the creation (annihilation) operator in the QD and U represents the intra-dot Coulomb repulsion between the s and p energy levels with i ($\bar{i}$)= s (p) or p (s). Finally, the third term $H_{\rm t}$ describes the tunneling part, which can be written as

$$H_{\rm t} = \sum_{\alpha;i=s,p} t_{\alpha,i} c^\dagger_{\alpha,k} d_i + {\rm H.c.}. \tag{3}$$

Here $t_{\alpha,i}$ are the hopping matrix elements between leads and two energy levels in InAs QD.

III. FORMULATION OF THE AVERAGE CURRENTS

Now, we implement the Keldysh non-equilibrium Green's function method to solve this model, which offers an efficient way to deal with many-body correlations in a unified fashion[23,24]. By applying this method to the irradiation problem, the time-dependent current from the left lead to the QD can be calculated from the evolution of the total number operator of the electrons in the left lead,

$$I_L(t) \equiv -e\langle \dot{n}_L \rangle = ie\langle [n_L, H(t)] \rangle \tag{4}$$

where $n_L = \sum_k c^\dagger_{L,k} c_{L,k}$ is the number operator of the electrons in the left lead. The total current can be written as a summation of the time-dependent left-going current through the s, p level respectively, i.e. $I_L(t) = \sum_{i=s,p} I^i_L(t)$, which is given by

$$I^i_L(t) = 2e{\rm Re}[t_{L,i} G^<_{i,L}(t,t)]. \tag{5}$$

Here, $G^<_{i,L}(t,t) \equiv i\langle c^\dagger_{L,k}(t) d_i(t)\rangle$ is the Keldysh Green function. With the help of the Dyson equation, $G^<_{i,L}(t,t)$ can be written as

$$G^<_{i,L}(t,t) = \int {\rm d}t_1 t^*_{L,i} [G^r_{i,i}(t,t_1) g^<_{kL}(t_1,t) + G^<_{i,i}(t,t_1) g^r_{kL}(t_1,t)], \tag{6}$$

where $G^r_{i,i}(t,t_1) \equiv -i\theta(t-t_1)\langle\{d_i(t), d^\dagger_i(t_1)\}\rangle$, $G^<_{i,i}(t,t_1) \equiv i\langle d^\dagger_i(t_1) d_i(t)\rangle$, and $g^<_{kL} = i f_L(\varepsilon - \mu_L)$, $g^r_{kL} = -i\theta(t-t_1)$ denote the less and retarded Green

functions of the electron in the left lead. Taking Eq. (6) into Eq. (5), we arrive at

$$I_L^i(t) = -2e\mathrm{Im}\int_{-\infty}^{t}\mathrm{d}t_1\int\frac{\mathrm{d}\varepsilon}{2\pi}e^{-i\varepsilon(t-t_1)} \Gamma_i^L(\varepsilon)[G_{i,i}^<(t,t_1)+f_L(\varepsilon)G_{i,i}^r(t,t_1)]. \quad (7)$$

Next, using the Keldysh equation $G_{i,i}^<(t,t') = \int\int \mathrm{d}t_1\mathrm{d}t_2 G_{i,i}^r(t,t_1)\Sigma_{i,i}^<(t_1,t_2)G_{i,i}^a(t_2,t')$ with $G_{i,i}^r = (G_{i,i}^a)^*$, the self-energy function $\Sigma_{i,i}^<(t_1,t_2) = i\int\frac{\mathrm{d}\varepsilon}{2\pi}e^{-i\varepsilon(t_1-t_2)}\sum_{\alpha=L,R}f_\alpha(\varepsilon-\mu_\alpha)\Gamma_i^\alpha$. Here, under the wide bandwidth approximation[25], the line width function $\Gamma_i^\alpha \equiv 2\pi\sum_\alpha t_{\alpha,i}t_{\alpha,i}^*\delta(\varepsilon-\varepsilon_{\alpha,k})$ is independent of energy.

Then, the time-dependent left-going current reduces to

$$I_L^i(t) = -e\Gamma_i^L\int\frac{\mathrm{d}\varepsilon}{2\pi}\sum_{\alpha=L,R}f_\alpha(\varepsilon-\mu_\alpha)|A_i^\alpha(\varepsilon,t)|^2 - e\Gamma_i^L\int\frac{\mathrm{d}\varepsilon}{2\pi}2f_L(\varepsilon-\mu_L)\mathrm{Im}A_i^L(\varepsilon,t), \quad (8)$$

where $f_\alpha(\varepsilon) = 1/(e^{\beta(\varepsilon-\mu_\alpha)}+1)$ denotes the Fermi distribution function of leads, and $A_i^\alpha(\varepsilon,t)$ is the spectral function which is given by

$$A_i^\alpha(\varepsilon,t) = \int_{-\infty}^{t}\mathrm{d}t_1 G_{i,i}^r(t,t_1)e^{-i\varepsilon(t_1-t)}. \quad (9)$$

For the two-terminal device, the average current of each level $\langle I_i\rangle \equiv \langle I_L^i(t)\rangle - \langle I_R^i(t)\rangle$ can be derived with the help of Eq. (8) as

$$\langle I_i\rangle = -2e\frac{\Gamma_i^L\Gamma_i^R}{\Gamma_i^L+\Gamma_i^R}\int\frac{\mathrm{d}\varepsilon}{2\pi}f_L(\varepsilon)\mathrm{Im}\langle A_i^L(\varepsilon,t)\rangle + 2e\frac{\Gamma_i^L\Gamma_i^R}{\Gamma_i^L+\Gamma_i^R}\int\frac{\mathrm{d}\varepsilon}{2\pi}f_R(\varepsilon)\mathrm{Im}\langle A_i^R(\varepsilon,t)\rangle, \quad (10)$$

and the total average current is $\langle I\rangle = \sum_{i=s,p}\langle I_i\rangle$.

The main step is then to determine the spectral function in Eq. (10). Note that, the spectral function is related to the retarded Green function $G_{i,i}^r$, which can be determined by the equation of motion (EOM)[26,27]. Here, we take the higher-order approximation to investigate the THz PATs and obtain

$$G_{i,i}^r(t,t') = [1-n_{\bar{i}}]g_{\varepsilon_i}^r(t,t')e^{-\frac{\Gamma_i}{2}(1-n_{\bar{i}})(t,t')} + n_{\bar{i}}g_{\varepsilon_i+U}^r(t,t')e^{-\frac{\Gamma_i}{2}n_{\bar{i}}(t,t')}, \quad (11)$$

where $g_{\varepsilon_i}^r(t,t') \equiv -i\theta(t-t')e^{-i\int_{t'}^{t}\varepsilon_i(\tau)\mathrm{d}\tau}$, and $g_{\varepsilon_i+U}^r(t,t') \equiv -i\theta(t-t')e^{-i\int_{t'}^{t}[\varepsilon_i(\tau)+U]\mathrm{d}\tau}$.

In the above equation, there are two kinds of resonances. In the first term, the resonances are at $\varepsilon_{s(p)}$, which occur when the $p(s)$ level is empty and there is no Coulomb interaction effect between the two levels. Whereas in the second term, the Coulomb interaction related resonances are at $\varepsilon_{s(p)}+U$, which can be understood as follows. First, in the case where p level is occupied, if another electron wants to transit through the s level, due to the Coulomb interaction U between the s and p levels, the energy of this electron becomes ε_s+U. On the other hand, in the case where s level is occupied, if another electron wants to transit through the p level, the resonance of this electron occurs at ε_p+U.

Taking the retarded Green function into the Eq. (9) gives rise to the following spectral function

$$A_i^\alpha(\varepsilon,t) = \sum_n J_n^2(\frac{W_d}{\omega})e^{in\omega t}\frac{1-n_{\bar{i}}}{\varepsilon-\varepsilon_i-n\omega+i\frac{\Gamma_i(1-n_{\bar{i}})}{2}} + \sum_n J_n^2(\frac{W_d}{\omega})e^{in\omega t}\frac{n_{\bar{i}}}{\varepsilon-\varepsilon_i-U-n\omega+i\frac{\Gamma_i n_{\bar{i}}}{2}}, \quad (12)$$

where J_n is the n-order Bessel function and n_i ($n_{\bar{i}}$) is the average electron occupation number of each energy level, which can be derived as

$$n_i = \langle d_i^\dagger d_i\rangle = \int\frac{\mathrm{d}\varepsilon}{2\pi}\sum_\alpha f_\alpha(\varepsilon)\Gamma_i^\alpha\langle|A_i^\alpha(\varepsilon,t)|^2\rangle. \quad (13)$$

Note that, in the two-level MWF QD, Coulomb interaction is much larger than the energy difference and can be regarded as infinite. Therefore, the second term of the spectral function Eq. (12) is ignored and only the first term contributes to the average currents. However, in InAs QD, because the intra-dot Coulomb interaction becomes comparable with the energy difference, the Coulomb blockade oscillations and related PATs arise from the second term, which is of equal importance as the first term and may present new features. To our knowledge, the finite U effects have not been explored theoretically in a InAs QD. Here for simplicity, we assume $\Gamma_i^L = \Gamma_i^R$ and define $\Gamma_i = \Gamma_i^L + \Gamma_i^R$. Then, by solving the Eqs. (12-13) self-consistently, one can obtain the average currents.

IV. RESULTS OF THE THZ PATS IN THE PRESENCE OF COULOMB INTERACTION

In this section, we present and discuss the main results of this work. We shall first analyze the tunneling experiment through a InAs QD based on the above formulation. Then, we explore the Coulomb interaction effects on the resonant tunnelings. To compare with the experiment, we consider the following parameters: $W_d = 0.9$, $\Gamma_s = 0.01$, $\Gamma_p = 0.03$, $k_BT = 0.1$, and $V = 0.02$ in our calculations.

A. Analysis of the experiment

In the experiment[22], the Coulomb charging energy $E_C = 15$ meV, which is comparable with the energy difference between s and p energy levels with $\Delta E = 5$ meV.

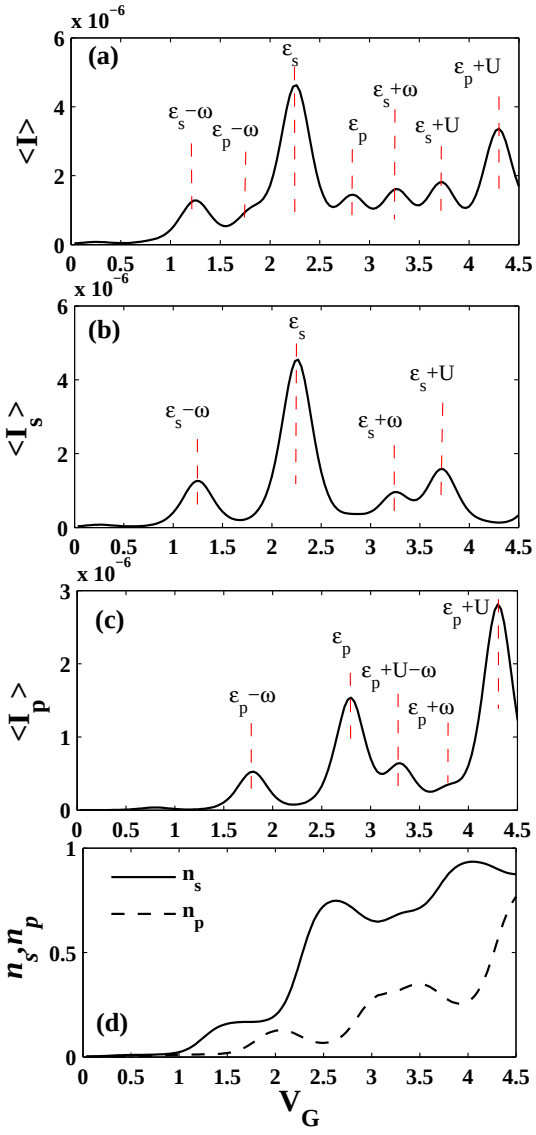

FIG. 2: (a) The total average current $\langle I\rangle$, and (b,c) the average current $\langle I_{s(p)}\rangle$ for $s(p)$ energy level as a function of the gate voltage V_G. (d) shows the average electron occupation number n_s and n_p. The intra-dot Coulomb interaction $U = 1.5$, $\Delta\varepsilon \equiv \varepsilon_p - \varepsilon_s = 0.5$, and the THz photon frequency $\omega = 1$.

the THz photon frequency is chosen to be larger than ΔE with $hf_{\rm THz} = 10.3$ meV. These parameters correspond to $U = 1.5$, $\Delta\varepsilon = 0.5$, and $\omega = 1$ ($\hbar = e = 1$) in the tunneling Hamiltonian (1). In Fig. 2, we plot the average currents and electron occupation number as a function of the gate voltage V_G. The main results are as follows.

First, in addition to the Coulomb blockade oscillation peaks ε_s and $\varepsilon_p + U$ as indicated in the experiment, there also exists $\varepsilon_s + U$ peak, see Fig. 2(a-b). In Fig. 2(d), we show that p energy level has a probability to be occupied. In this case, when an electron tries to transit through the s level, it will be accompanied by a Coulomb repulsion U. Therefore, for $V_G = \varepsilon_s + U$, a resonant tunneling occurs.

Secondly, the photon-assisted side peaks at $\varepsilon_s \pm \omega$ can be observed, with the right side peak $\varepsilon_s + \omega$ in $\langle I_s\rangle$ reduced slightly due to the competition with the nearby $\varepsilon_s + U$ peak (Fig. 2(b)). However, in the total average current $\langle I\rangle$, the $\varepsilon_s + \omega$ peak coincides with the Coulomb blockade oscillation PAT $\varepsilon_p + U - \omega$ in Fig. 2(c), leading to the enhancement of this peak.

Thirdly, without THz irradiation, because of the Coulomb blockade, the ε_p peak is strongly suppressed. Whereas under the THz irradiation, an electron in s level can be excited into leads, which reduces the Coulomb repulsion of p level and results in the subsequent tunneling of electrons from leads through p level, see the PIER peak of ε_p in Fig. 2(a,c).

Finally, there exist two side peaks at $\varepsilon_p \pm \omega$ in Fig. 2(c). For $V_G = \varepsilon_p - \omega$, both energy levels are above the chemical potential of leads, an electron can tunnel through p level with the help of THz irradiation and one can observe the PAT peak in the total average current (Fig. 2(a)). Whereas for $V_G = \varepsilon_p + \omega$, the two energy levels are below the chemical potential of leads. In this case, the energy separation between s level and leads is $\omega + \Delta\varepsilon$, which is larger than the THz photon frequency ω. So, it is hard to excite an electron in s level into leads, and results in a suppression of this side peak.

We now compare the above results with the InAs QD experiment. We show that, the presented peaks of our model analysis ε_s, $\varepsilon_p + U$, $\varepsilon_s \pm \omega$, ε_p agree well with E_0, E_1, $E_0 \pm hf_{\rm THz}$, and the PIER of p level in Fig. 3 of the reference[22]. We find the side peak $\varepsilon_p - \omega$ induced by the THz irradiation in our model analysis. This peak can be identified in the original experimental data, but was not addressed in the reference[22]. In addition, beyond the Coulomb blockade oscillation peak $\varepsilon_p + U$, we also find there exists the $\varepsilon_s + U$ peak. This peak seems not readily discriminated from E_1 ($E_1 \equiv \varepsilon_p + U$) peak in the experiment. In the future, one may expect to identify both the peaks $\varepsilon_{s,p} + U$ by increasing the separation between the energies ε_s and ε_p.

We then compare our results with the MWF QD[2,28]. We see that beyond the PAT resonances of the two levels in MWF QD, the Coulomb blockade oscillation peaks of $\varepsilon_{s,p} + U$ appear in the InAs QD. Moreover, we find that the photon-assisted tunnelings of these Coulomb blockade oscillation peaks occur, which also contribute to the side peaks of the s level, see below for detailed discussions.

B. Coulomb interaction effects on the resonant tunnelings

Now, we explore systematically the Coulomb interaction effects on the resonant tunnelings. We first consider $\Delta\varepsilon < \omega < U$. Fig. 3 shows the results of the average currents for $U = 1.5$ and 3. We see that, while the main resonance ε_s, the PIER of ε_p, and the side peaks $\varepsilon_{s,p} \pm \omega$ are not affected by increasing U, the Coulomb interaction

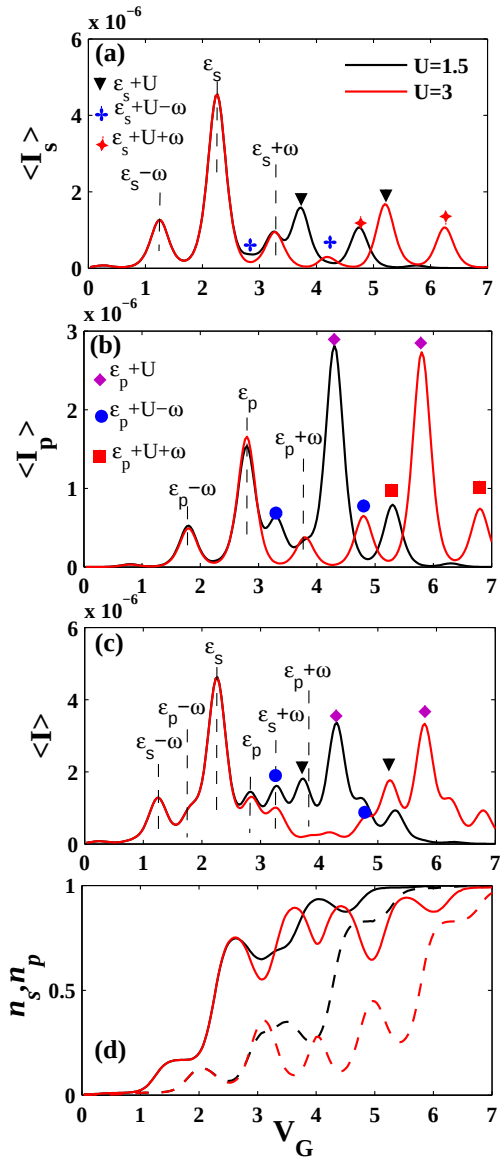

FIG. 3: (color online) (a,b) The average current $\langle I_{s(p)}\rangle$ for $s(p)$ energy level, and (c) the total average current $\langle I\rangle$ as a function of the gate voltage V_G for $\Delta\varepsilon < \omega < U$. (d) shows the average electron occupation number n_s (solid lines) and n_p (dashed lines).

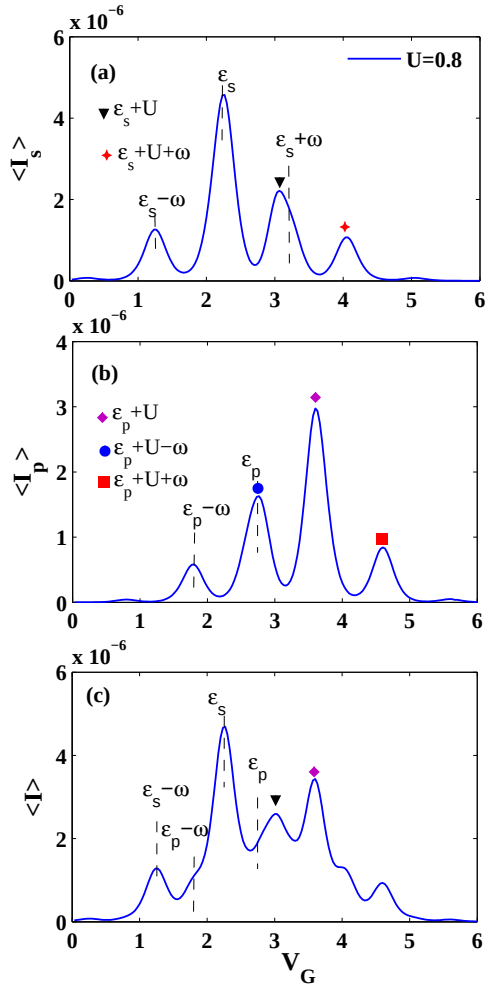

FIG. 4: (color online) (a,b) The average current $\langle I_{s(p)}\rangle$ for $s(p)$ energy level, and (c) the total average current $\langle I\rangle$ as a function of the gate voltage V_G for $\Delta\varepsilon < U < \omega$.

involved resonances, like the peaks $\varepsilon_{s,p}+U$, and related PATs $\varepsilon_{s,p}+U\pm\omega$ shift to higher gate voltage, but the strengthen remains almost unchanged. Significantly, the Coulomb blockade oscillation PATs $\varepsilon_s+U\pm\omega$ are asymmetric with the peak $\varepsilon_s+U-\omega$ being largely suppressed (Fig. 3(a)). This is because the occupation number n_p for $V_G = \varepsilon_s+U-\omega$ is much smaller compared with $V_G = \varepsilon_s+U+\omega$ (see $U=3$ in Fig. 3(d) for example), which makes an electron have little probability to transit into the energy level ε_s+U and thus reduces the PAT. On the other hand, the Coulomb blockade oscillation PATs $\varepsilon_p+U\pm\omega$ are quite symmetric, as shown in Fig. 3(b).

In Fig. 3(c), we plot the total average current $\langle I\rangle$ versus the gate voltage V_G. The tunneling processes can be divided into three regimes, see $U=3$ for example. For the low gate voltage $V_G \le \varepsilon_s+\omega$, we can observe the main resonance ε_s, the PIER of ε_p, and the related side peaks $\varepsilon_s\pm\omega$ or $\varepsilon_p-\omega$. For the high gate voltage $V_G \ge \varepsilon_s+U$, the peaks $\varepsilon_{s,p}+U$ become the dominant tunneling processes. Whereas for V_G between above two regimes, one enters into the Coulomb blockade regime, where the finite total average current arises from the side peak $\varepsilon_p+\omega$ and Coulomb blockade oscillation PATs like $\varepsilon_{s,p}+U-\omega$.

Finally, we discuss the Coulomb interaction effects for $\Delta\varepsilon < U < \omega$. In this case, the peaks ε_s+U (Fig. 4(a)) and ε_p+U (Fig. 4(b)) now move to the low gate voltage regime and merge with the side peak $\varepsilon_s+\omega$, making this side peak hard to be distinguished. Significantly, although one can see the PIER of ε_p in the average current $\langle I_p\rangle$ (Fig. 4(b)), because ε_s+U now dominates the tunneling process and lies very close to p level, the PIER of ε_p can not be directly identified, see Fig. 4(c). Further-

more, while the main resonance ε_s, and the side peaks $\varepsilon_{s,p} - \omega$ are not affected, the Coulomb blockade oscillation PATs $\varepsilon_{s,p} + U - \omega$ become featureless.

V. CONCLUSION

In conclusion, we have explored the THz photon-assisted tunneling through a two-level InAs QD. Because the Coulomb interaction is of the same order as the THz energy difference, the finite Coulomb interaction plays important roles on the tunneling processes. We demonstrate that, the Coulomb blockade oscillation and PIER of p level can be clearly observed. Beyond these results, we find new Coulomb blockade oscillation and PAT peaks, which may be identified in further experiment. In particular, we find that, to observe the interesting photon-induced excited state resonance of p level, the Coulomb interaction should be larger than THz photon frequency. We believe these features are of practical importance for future THz devices, for example, developing a highly sensitive and frequency-tunable THz detector.

This work is supported by NCET, NSFC under grants Nos. 11174168, 11074175, NKBRSFC under grants No. 2011CB606405, and National Special Fund for the Development of Major Research Equipment and Instruments under grants No. 2011YQ13001805.

* Electronic address: sunqing@iphy.ac.cn
† Electronic address: andrewjee@sina.com

[1] L. P. Kouwenhoven, S. Jauhar, J. Orenstein, P. L. McEuen, Y. Nagamune, J. Motohisa, and H. Sakaki, Phys. Rev. Lett. **73**, 3443 (1994).
[2] T. H. Oosterkamp, L. P. Kouwenhoven, A. E. A. Koolen, N. C. van der Vaart, and C. J. P. M. Harmans, Phys. Rev. Lett. **78**, 1536 (1997).
[3] T. Fuse, Y. Kawano, M. Suzuki, Y. Aoyagi, K. Ishibashi, Appl. Phys. Lett. **90**, 013119 (2007).
[4] J. R. Tucker and M. J. Feldman, Rev. Mod. Phys. **57**, 1055 (1985).
[5] T. Yamamoto, Y. A. Pashkin, O. Astafiev, Y. Nakamura, and J. S. Tsai, Nature **425**, 941 (2003).
[6] T. Hayashi, T. Fujisawa, H. D. Cheong, Y. H. Jeong, and Y. Hirayama, Phys. Rev. Lett. **91**, 226804 (2003).
[7] J. R. Petta, A. C. Johnson, J. M. Taylor, E. A. Laird, A. Yacoby, M. D. Lukin, C. M. Marcus, M. P. Hanson, and A. C. Gossard, Science **309**, 2180 (2005).
[8] F. H. L. Koppens, C. Buizert, K. J. Tielrooij, I. T. Vink, K. C. Nowack, T. Meunier, L. P. Kouwenhoven, and L. M. K. Vandersypen, Nature **442**, 766 (2006).
[9] G. Platero and R. Aguado, Phys. Rep. **395**, 1 (2004).
[10] A. Goker and E. Gedik, arXiv:1303.2859.
[11] F. R. Braakman, P. Barthelemy, C. Reichl, W. Wegscheider, and L. M. K. Vandersypen, Appl. Phys. Lett. **102**, 112110 (2013).
[12] T. Kwapiński, R. Taranko, and E. Taranko, Phys. Rev. B **72**, 125312 (2005).
[13] W. G. van der Wiel, S. De Franceschi, J. M. Elzerma, T. Fujisawa, S. Tarucha, and L. P. Kouwenhoven, Rev. Mod. Phys. **75**, 1 (2002).
[14] T. Frey, P. J. Leek, M. Beck, A. Blais, T. Ihn, K. Ensslin, and A. Wallraff, Phys. Rev. Lett. **108**, 046807 (2012).
[15] C. Bergenfeldt and P. Samuelsson, Phys. Rev. B **85**, 045446 (2012).
[16] B. Ferguson and X.-C. Zhang, Nat. Mater. **1**, 26 (2002).
[17] M. Tonouchi, Nat. Photonics **1**, 97 (2007).
[18] T. Fuse, Y. Kawano, T. Yamaguchi, Y. Aoyagi, and K. Ishibashi, Nanotechnology **18**, 044001 (2007).
[19] Y. Kawano, T. Fuse, S. Toyokawa, T. Uchida, and K. Ishibashi, J. Appl. Phys. **103**, 034307 (2008).
[20] M. Jung, T. Machida, K. Hirakawa, S. Komiyama, T. Nakaoka, S. Ishida, and Y. Arakawa, Appl. Phys. Lett. **87**, 203109 (2005).
[21] K. Shibata, M. Jung, K. M. Cha, M. Sotome, and K. Hirakawa, Appl. Phys. Lett. **94**, 162107 (2009).
[22] K. Shibata, A. Umeno, K. M. Cha, and K. Hirakawa, Phys. Rev. Lett. **109**, 077401 (2012).
[23] N. S. Wingreen, A. P. Jauho, and Y. Meir, Phys. Rev. B **48**, 8487 (1993).
[24] A. P. Jauho, N. S. Wingreen, and Y. Meir, Phys. Rev. B **50**, 5528 (1994).
[25] N. S. Wingreen, K. W. Jacobsen, and J. W. Wilkins, Phys. Rev. B **40**, 11834 (1989).
[26] Q. F. Sun, J. Wang, and H. Guo, Phys. Rev. B **71**, 165310 (2005).
[27] G. Hackenbroich and H. A. Weidenmuller, Phys .Rev. Lett. **76**, 110 (1996).
[28] Q. F. Sun, J. Wang, T. H. Lin Phys. Rev. B **58**, 13007 (1998).